

THE EFFECT OF TEMPERATURE ON THE STRAIN-INDUCED AUSTENITE TO MARTENSITE TRANSFORMATION IN SS 316L DURING UNIAXIAL TENSION

Elizabeth M. Mamros^{1*}, M. Bram Kuijer², Mohammad Ali Davarpanah¹, Ian Baker², and Brad L. Kinsey¹

¹University of New Hampshire, Durham, NH, 03824, USA

²Dartmouth College, Hanover, NH, 03755, USA

*Corresponding Author, emm1109@wildcats.unh.edu

Keywords: Forming, Uniaxial tension, Martensitic transformation, Stainless steel

Abstract

Controlling the microstructure of components is of interest to achieve optimal final part properties, i.e., materials by design. The manufacturing process itself can affect a material's characteristics by changing the microstructure. For example, past research has shown that an austenite to martensite phase transformation in stainless steel occurs during deformation. Temperature is known to have a significant influence on this phenomenon. In this paper, the effect of temperature on the austenitic to martensite phase transformation in SS 316L under uniaxial tension is investigated. Both a cooling system and a heat exchanger were employed in a uniaxial tension experimental setup to control the temperature. Tensile specimens were strained to fracture at four temperatures of -15°C, 0°C, 10°C, and 20°C. Digital imaging correlation (DIC) and a thermal imaging camera were used for tests at 0°C and above to capture strain and temperature data, respectively. Strain data could not be obtained at -15°C due to the DIC paint flaking during testing. X-ray diffraction was used to measure the weight percent of martensite in both the as-received and the tensile-tested materials.

1. Introduction

One means to achieve optimal final part properties during forming is by controlling the microstructure of materials. However, this objective is extremely complex due to the number of variables involved, including temperature, strain rate, stress-strain state, and deformation path, and their interdependence [1].

A microstructural phase transformation to martensite occurs during forming in austenitic stainless steels (SS) at room temperature. This effect is increased at temperatures below zero Centigrade and at high strains [2]. Hecker et al. found that at strains <0.25, high strain rates produced more martensite, while the converse occurred at larger strains [1]. Thus, for uniaxial tensile tests of ductile materials, low strain rates and low temperatures are preferred to obtain a larger weight percentage of martensite.

As is typical for all metals and alloys, austenitic SS exhibits plasticity-induced heating. Nonhomogeneous deformation along the gauge length and heat conduction from the center towards the ends of the specimen leads to temperature gradients which affect the amount of martensitic transformation. The weight percent of martensite increases

from the end of the gauge length towards the center in deformed specimens [3]. Huang et al. [4] found that at temperatures $>50^{\circ}\text{C}$, martensite is not present. At -70°C , the martensitic transformation rate reaches a maximum at approximately 0.15 strain. As the temperature increases towards room temperature, the maximum martensitic transformation rate decreases and occurs at higher strains.

At low temperatures between approximately -80°C and -50°C , the strength increases rapidly due to the high rate of martensitic transformation at low strains. Due to the large amount of martensite near the beginning of the forming process, the strain hardening rate suddenly decreases at higher strains. If the temperature is approximately 25°C , then the rate of martensitic transformation is lower at low strains but occurs over a larger range of strains. This leads to a lower rate of increase in flow stress due to martensitic transformation and a more gradual decrease in the strain hardening rate at high strains. Consequently, maximum uniform elongation occurs around 0°C [4].

Moser et al. [5] conducted isothermal uniaxial tension tests for SS 304 specimens at temperatures ranging from 0°C to 100°C and found the largest weight percent of martensite in the 0°C specimens. Therefore, additional experiments are required at subzero temperatures to verify that the weight percent of martensite continues to increase with decreasing temperature.

In this paper, results from “isothermal” uniaxial tensile tests on SS 316L specimens are presented for temperatures ranging from -15°C to 20°C (room temperature). (Note that a temperature gradient exists just prior to fracture so the test is not truly isothermal.) To investigate the temperature effect on martensitic phase transformation, x-ray diffraction (XRD) was used, and the resulting weight percentages were compared for the formed specimens. Digital Image Correlation (DIC) and thermal imaging were used to measure strain and temperature, respectively, for tests with a temperature above 0°C . The required speckle pattern was not able to withstand the subzero temperature conditions due to paint flaking. Based on previous work, the hypothesis is that the weight percent of martensite will increase with decreasing temperature.

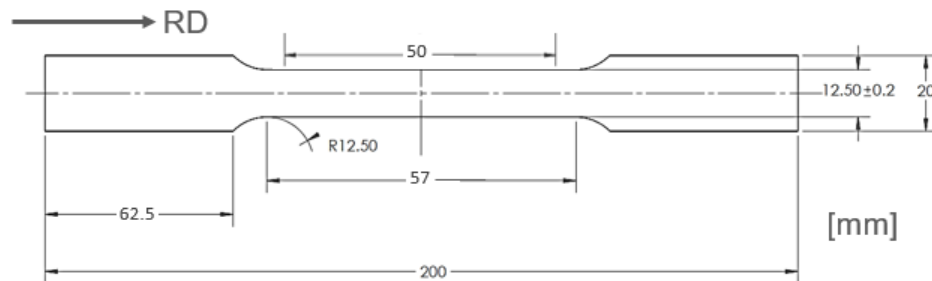


Figure 1. ASTM E8 specimens obtained from 1.2 mm thick SS 316L.

2. Experimental Setup and Methods

2.1 Material and Specimen Preparation

Dogbone specimens, dimensioned according to the ASTM E8 standard, were waterjet cut from SS 316L, 1.2 mm thick sheets with the 57 mm gauge length oriented along the rolling direction (Figure 1). Due to the rough surfaces created by waterjet cutting, the edges were sanded, and the initial width and thickness were measured with a caliper and micrometer, respectively, prior to testing.

2.2 Cooling System

A cooling system, which consisted of a compressor (Thermo Fisher), pump (Thermo Fisher), and cold plate (AAVID), was used with a 60% ethylene glycol/40% water mixture to create “isothermal” testing conditions. The cooling system temperature range is -50°C to 200°C, but the lower threshold for the ethylene glycol/water coolant is -30°C. The temperature range of the cold plate is -65°C to 155°C. To account for heat transfer, the temperature setting for the cooling system was adjusted accordingly to ensure that the specimen reached the desired steady-state temperature prior to each experiment. The specimen temperature was verified with a thermocouple.

2.3 Experimental Setup

A MTS Landmark machine was utilized to perform the uniaxial tension tests. A pulling speed of 0.1 mm/s was used, which produced an initial strain rate of $\sim 1 \times 10^{-3} \text{ s}^{-1}$. The cold plate was clamped to the bottom half of each specimen in the grip area and remained stationary during the experiment (Figure 2). A small force was applied out-of-plane behind the cold plate to create uniform contact across the entire specimen gauge area for the duration of the test. A piece of cork board was used to ensure that no contact occurred between the MTS grips and the cold plate.

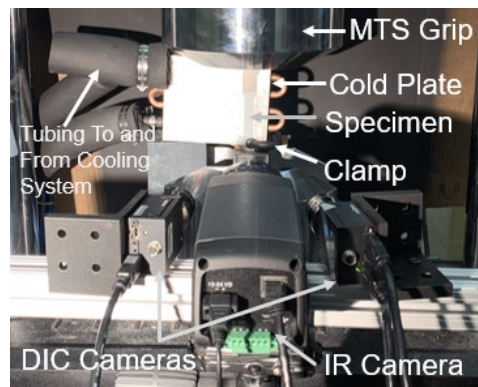


Figure 2. Experimental setup with DIC, IR camera, cooling system, and MTS grips.

2.4 Digital Image Correlation and Thermal Camera

To capture local strains *in-situ*, two FLIR 5.0 megapixel cameras with 17 mm Schneider Xenoplan compact lenses were setup for three-dimensional DIC (Figure 2). To create the contrast required for this technique, a white background with a black speckle pattern in the foreground was created with spray-paint. All images were post-processed with subset and step sizes of 17 and 4 respectively in VIC-3D (Correlated Solutions Inc.). An area slightly larger than the 57 mm gauge length was selected for the analyses.

Coupled with the DIC cameras in VIC Snap, the image capturing software from Correlated Solutions Inc., a FLIR SC-645 infrared (IR) camera was used to measure the temperature during the tests. The infrared camera has a temperature range of -20°C to 650°C with a temperature resolution of 0.05°C. The spatial resolution is 640 x 480 pixels.

2.5 Martensitic Transformation Measurements

A Rigaku 007 XRD was utilized to measure the weight percent of the BCC phase, or martensite. A 2θ range of $30\text{-}140^\circ$ was used in order to collect all the relevant martensite peaks. The scan was performed with a count time of 3 seconds and a step of 0.050° using a voltage and current of 40 kV and 300 mA, respectively. The divergence slit and receiving slit widths and angles were set to 1.22 mm, 0.3 mm and 2° , 2° respectively. Each specimen was ground using a polishing wheel with 600-grit SiC paper to create a flat surface as required for the XRD. A large water flow was used to eliminate a heat-induced phase change and damage during polishing. JADE software (Material Data, Inc.) was used to determine the weight percent of the FCC (austenite) and the BCC (martensite) phases in each specimen. The angular slack to shift was set at $\Delta 2\theta \pm 0.18^\circ$.

3. Results and Discussion

3.1 Temperature

Figure 3 shows the strain and temperature distributions from the last image captured by the DIC and IR camera prior to fracture for the 0°C , 10°C , and 20°C specimens. Table 1 shows the corresponding true strain and temperature values at a point located in the center of the fracture location. Neither DIC nor IR data could be captured from the -15°C specimens as the paint used to provide the speckle pattern lost adhesion at subzero temperatures.

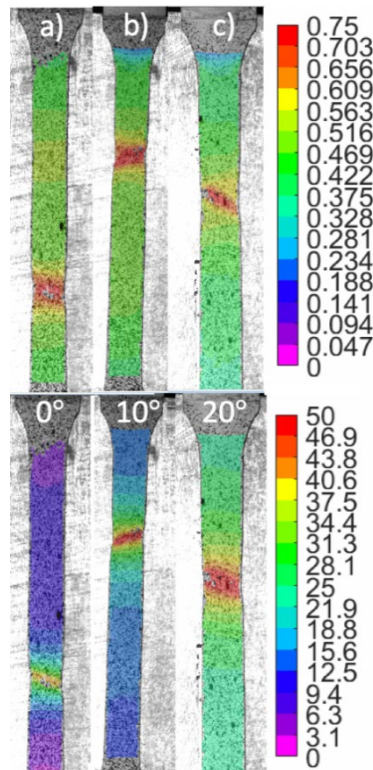


Figure 3. True strain (top) and temperature (bottom) distributions prior to fracture for a) 0°C , b) 10°C , and c) 20°C specimens.

Table 1. DIC and IR results from uniaxial tests.

| Specimen | True strain just before fracture | Temperature just before fracture (°C) |
|----------|----------------------------------|---------------------------------------|
| 0°C | 0.721 | 42.74 |
| 10°C | 0.805 | 45.90 |
| 20°C | 0.733 | 56.05 |

From Figure 3, it is evident that the cold plate is able to maintain nearly isothermal conditions near the ends of the specimen throughout the duration of the test. However, the gauge section still undergoes plasticity-induced heating and reaches gradients up to approximately 30°C across the 57 mm gauge length for the room temperature experiments. This heating occurs rapidly as the specimen approaches fracture (Figure 4), because the cold plate is no longer sufficient to maintain an isothermal temperature. The sequential frame numbers and strain values are provided in Figure 4 to show that the temperature increase is primarily at the end of the test as the strain localization occurs.

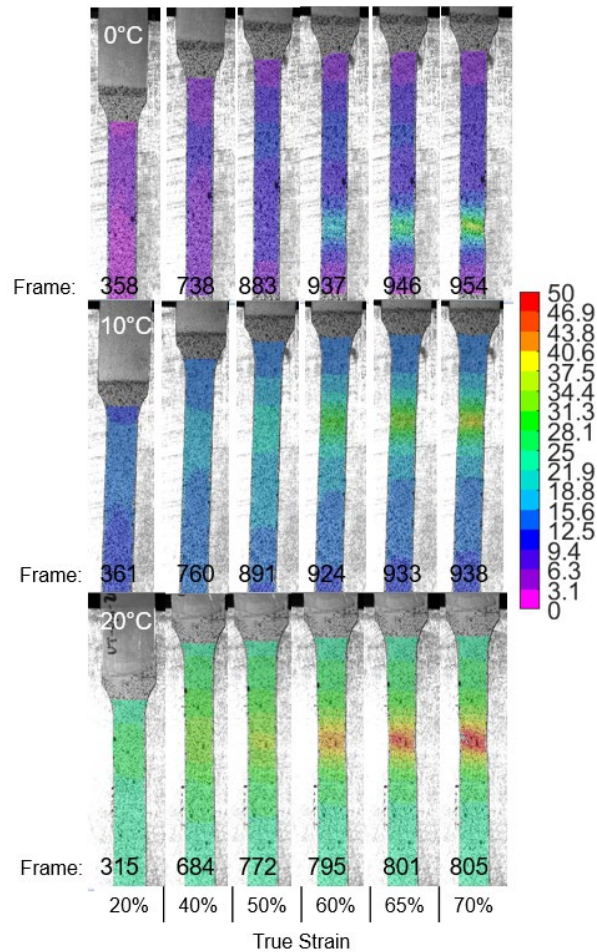


Figure 4. Temperature distribution (°C) over time (represented by frame number) for 0°C (top), 10°C (middle), and 20°C (bottom) specimens.

3.2 Stress-Strain Curves

Since DIC data is not available for -15°C experiments, engineering stress versus plastic strain curves were created using the MTS cylinder location data for the strain calculation (Figure 5). A general trend of increased engineering flow stress as the temperature decreases occurs from 20°C to -15°C (although the 0 and -15°C curves are nearly identical). This is consistent with results in Huang et al. [4] although the temperature effect persisted for sub-zero temperatures in their research. In addition, Figure 4 shows that the 0°C experiment has the highest elongation, which also matches the results in Huang et al. [4]. This strain data represents the deformation over the entire gauge area with the engineering stress calculated from the initial specimen cross-section. As shown in Figure 3 though, the strain localizes in the necked region of the specimen during the tests.

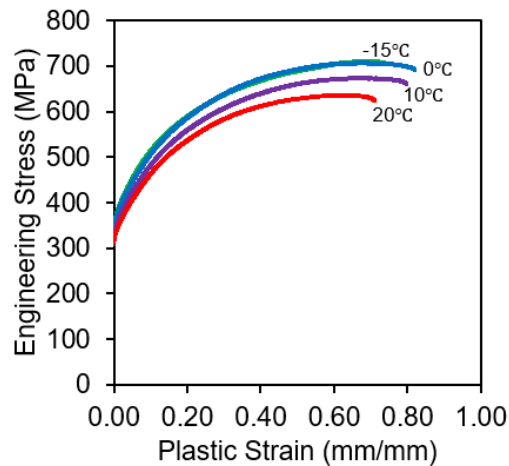


Figure 5. Engineering Stress-Plastic Strain for -15°C , 0°C , 10°C , and 20°C tests.

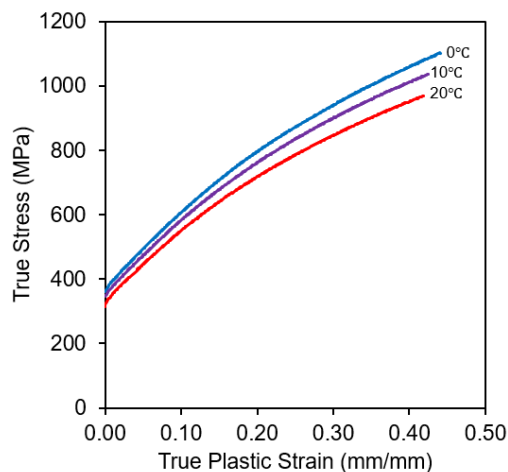


Figure 6. True Stress-True Plastic Strain curves for 0°C , 10°C , and 20°C tests.

DIC allows the strain in the fracture region to be assessed and the stress to be calculated based on the instantaneous gauge area, i.e., the true stress, up to localized necking. Figure 6 shows the true stress-true strain curves for specimens tested at 0°C , 10°C , and 20°C . As is evident, the temperature effect of Figure 5 is also present when probing data

in the fracture location. While at least three specimens have already been tested at each temperature, additional trials will be conducted to assure consistency of this data.

3.3 Martensitic Transformations

Table 2 shows the weight percentages of martensite for the formed specimens measured near the fracture location. This follows the expected trend that the weight percent of martensite increases near the fracture location with decreasing temperature. The increased martensite causes the higher stress values as seen in Figure 5. As anticipated, the as-received material shows no martensite present so the plasticity-induced austenite to martensite transformation occurs at all temperatures investigated.

Table 2. Martensite weight percentages from XRD near fracture location.

| Temperature | Weight Percent |
|--------------------|-----------------------|
| -15°C | 58.2% |
| 0°C | 26.1% |
| 10°C | 17.8% |
| 20°C | 13.1% |

4. Conclusion and Future Work

SS 316L specimens were loaded in uniaxial tension until fracture under nearly isothermal conditions at -15°C, 0°C, 10°C, and 20°C. XRD measurements showed that reducing the temperature increases the weight percentage of martensite in the tested specimens at the fracture location. Future experiments could include a different method of creating isothermal conditions, e.g., an enclosed cooling system, to further reduce the observed plasticity-induced heating effects. Alternatively, a different coolant could be used with the current cooling system to perform additional experiments at even lower temperatures. Electron backscatter diffraction (EBSD) will be used to verify the martensite weight percentages. In the future, crystal plasticity modeling will be implemented to provide a fundamental understanding of the phase transformation mechanisms and determine optimal deformation paths to intentionally manipulate final material properties.

5. Acknowledgements

Support for the NH BioMade Project is provided by the National Science Foundation through the EPSCoR Research Infrastructure Improvement Award #1757371. Special appreciation to Marguerite Kennish for her assistance with uniaxial tension testing and processing the data.

6. References

- [1] Hecker, SS, Stout, MG, Staudhammer, KP, and Smith, JL. (1982) Effects of Strain State and Strain Rate on Deformation-Induced Transformation in 304 Stainless Steel: Part I. Magnetic Measurements and Mechanical Behavior. Metallurgical Transactions A, 13A: 619-26.
- [2] Lichtenfeld, JA, Van Tyne, CJ, and Mataya, MC. (2006) Effect of strain rate on stress-strain behavior of alloy 309 and 304L austenitic stainless steel. Metallurgical and Materials Transactions A. 37: 147. doi.org/10.1007/s11661-006-0160-5
- [3] Kumar, A and Singhal, LK. (1989) Effects of strain state and strain rate on deformation-induced transformation in 304 stainless steel: Part I. Magnetic measurements and mechanical behavior. Metallurgical and Materials Transactions A. 20: 2857. doi.org/10.1007/BF02670178
- [4] Huang, GL, Matlock, D & Krauss, G. (1989) Martensite formation, strain rate sensitivity, and deformation behavior of type 304 stainless steel sheet. Metallurgical and Materials Transactions A. 20: 1239. doi.org/10.1007/BF02647406
- [5] Moser, NH, Gross, TS & Korkolis, YP. (2014) Martensite formation in conventional and isothermal tension of 304 austenitic stainless steel measured by x-ray diffraction. Metallurgical and Materials Transactions A. 45: 4891. doi.org/10.1007/s11661-014-2422-y